Rev.Adv.Mater.Sci. 25 (2010) 261-269

MICROSTRUCTURE, CORROSION AND WEAR BEHAVIOUR OF UFG-POWDER-METALLURGICAL Al-Cu ALLOYS, Al-Cu/Al_2O_3(p) AND Al-Cu/SiC(p) COMPOSITES

D. Nickel, G. Alisch, H. Podlesak, M. Hockauf, G. Fritsche and T. Lampke

Institute of Materials Science and Engineering, Chemnitz University of Technology, Erfenschlager Str. 73, D-09125 Chemnitz, Germany

Received: November 28, 2009

Abstract. The effect of severe plastic deformation on the corrosion and wear behaviour of composites has been studied. The composites based on an Al-Cu alloy (EN AW-2017) processed by powder metallurgy were severely plastically deformed using equal-channel angular pressing (ECAP) to produce an ultrafine-grained (UFG) microstructure. Al_2O_3 or SiC particles in two different fractions (5 or 15 vol.%) as well as sizes (fine or nano) were used as reinforcements.
The corrosion behaviour was evaluated by potentiodynamic polarization in NaCl solution. X-ray diffraction reveals the development of the texture as a function of ceramic particle fraction and introduction of massive plastic deformation. In agreement with [1], the multiphase material without additional heat supply shows no deterioration in the corrosion characteristics after ECAP.
The wear behaviour was evaluated by oscillating friction and wear as well as scratch tests. The reinforced non-ECAP composites are more resistant against an oscillating friction movement whereas under abrasive load, the ECAP conditions behave the opposite.

1. INTRODUCTION

Microstructure, corrosion and wear behaviour of UFG-powder-metallurgical Al-Cu alloys, Al-Cu/Al_2O_3(p) and Al-Cu/SiC(p) composites are the objects of investigation for the presented study. Severe plastic deformation can be realized using equal-channel angular pressing (ECAP) to produce an ultrafine-grained (UFG) microstructure, for example [2].

It is known that severely plastically deformed multiphase alloys like Al-Mg-Si offer higher corrosion resistance as well as strength, for instance [1,3]. It could be clearly shown that fragmented and redistributed metallographic constituents (or impurities) are responsible for the observed effect. The cited works present investigations without additional tempering after SPD. This fact becomes important because of the ability of the material for artificial ageing.

The general idea of adding particles is to reinforce and strengthen the material further. Mechanical and wear properties like strength and abrasion resistance of these composites can be significantly improved compared to the matrix phase [4]. At the

Corresponding author: D. Nickel, e-mail: daniela.nickel@mb.tu-chemnitz.de

same time, however, these reinforcements increase the corrosion susceptibility of composites such as aluminium matrix composites, which is raised by the different corrosion behaviour of the combined materials, the emerging interfacial characteristics (e.g. condition of manufacturing-based phases), higher dislocation density and finally by the resulting less stable natural oxide film [5,6].

Any lack of information concerning the effect of ECAP on the corrosion and wear behaviour of composites justifies the topic of the present paper: to investigate the influence of ECAP in combination with different heat treatment procedures on Al-Cu composites with differences in type and size of the used reinforcements.

2. EXPERIMENTAL PROCEDURE

2.1. Material and processing

An Al-Cu alloy containing 0.7 wt.% Mg, 0.6 wt.% Mn, 3.9 wt.% Cu, and balance Al (equivalent to EN AW-2017 with lowered Si content) serves as matrix phase of the powder-metallurgically produced composites. As reinforcement, common particles such as SiC and Al_2O_3 with contents of 5 or 15 vol.%, respectively, were chosen. The size of the particle ranges from 0.2 to 2 μm (fine fraction). Additionally, SiC particles smaller than 0.2 μm (nano fraction) were used.

After high-energy ball milling (3 h), the compacted material (isostatic pressing, degassing in nitrogen atmosphere and direct extrusion) was exposed to different thermomechanical treatments. The ECAP processing was performed on billets of 15 x 15 mm^2 in cross-section and 120 mm in length in a hateable die-set with an intersection angle of 120°. The friction conditions inside the die are optimized by two movable walls in the inlet channel and a moving bottom slider in the outlet channel according to [7]. To ensure a fully homogeneous deformation and to suppress shear localisations or even cracks an active backpressure of 300 MPa was applied via the moving bottom slider. The experiments were performed at 50 mm min^{-1} for one pass (produces an equivalent plastic strain of ~0.67) following two different concepts. The first one includes processing at room temperature in order to introduce the deformation prior to aging. Conditions produced following this concept are designated with -W-E1-T4 hereafter. The second concept includes processing at 180 °C in the water quenched and artificially aged condition (170 °C for 20 min). The designation for these conditions hereafter is -T61-E1-180. Further details on the heat treatments and processing can be found in [8] (see TMT-2 and -4).

Table 1 presents the details of the investigated materials. Thereby in each case, the naturally aged conditions (T4) serve as reference for the ECAP conditions. As an example Fig. 1 presents the microstructure by means of the scanning transmission electron microscopy (STEM) of the composite with 15 vol.% Al_2O_3 before and after ECAP. It is obvious that in the non-ECAP material the grain size of the matrix phase shows an irregular distribution of larger and smaller grains. The smaller grains can be found near the area with many particles and measure around 1 μm. Detailed information about the comparison between the metallic and mixing zone are described in [9]. After one ECAP pass the microstructure maintain heterogeneously. In the area with a high fraction of reinforcement the grain size is less than 100 nm and globular, whereas in the almost particle-free zone the grains are elongated (length ~300 nm, width ~100 nm).

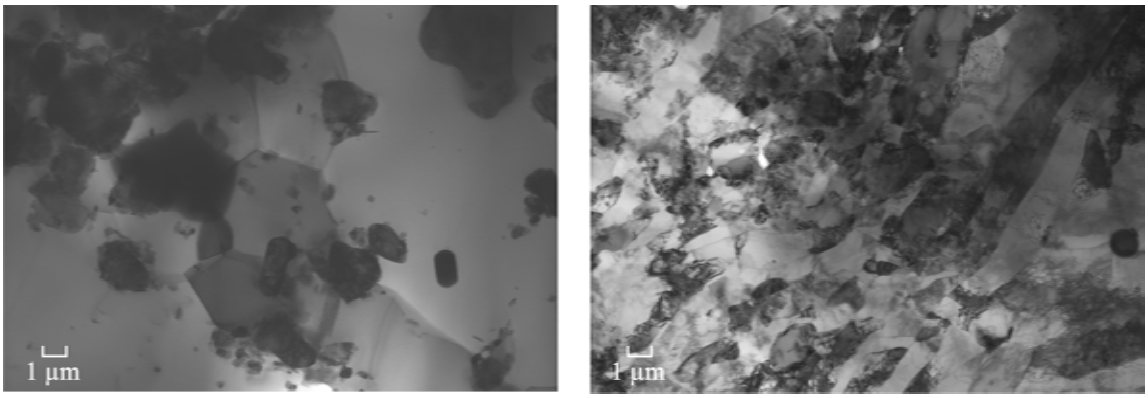

Fig. 1. STEM (LV) micrographs of the Al-Cu alloy with 15 vol.% Al_2O_3 particles (left:non-ECAP condition, right: ECAP condition).

Table 1. Designation of the investigated samples and their processing details (CIP - cold isostatic pressing; HIP - hot isostatic pressing; W-E1-T4 - solid-solution heat treatment at 505 °C for 60 min followed by water quenching, one ECAP-pass at room temperature; T61-E1-180 - solid-solution heat treatment at 505 °C for 60 min followed by water quenching and artificial ageing at 170 °C for 20 min, one ECAP-pass at 180 °C).

non-ECAP		ECAP		
		without reinforcement		
2017	(CIP)-T4	2017	-W-E1-T4	(CIP)
		+ Al_2O_3 (fine, 0.2 ... < 2 μm)		
2017 + 5 vol.%	(HIP)-T4	2017 + 5 vol.%	-W-E1-T4	(HIP)
2017 + 15 vol.%	(HIP)-T4	2017 + 15 vol.%	-W-E1-T4	(HIP)
		+ SiC (fine, 0.2 ... < 2 μm)		
2017 + 5 vol.%	(HIP)-T4	2017 + 5 vol.%	-W-E1-T4	(HIP)
		+ SiC (nano, < 0.2 μm)		
2017 + 5 vol.%	(HIP)-T4	2017 + 5 vol.%	-T61-E1-180	(HIP)
		+ SiC (fine, 0.2 ... < 2 μm)		
2017 + 15 vol.%	(HIP)-T4	2017 + 15 vol.%	-T61-E1-180	(HIP)

The samples were prepared by cutting mechanically in the extrusion direction, followed by polishing.

2.2. Corrosion behaviour

The corrosion susceptibility of the ECAP samples (working electrode) was examined by potentiodynamic polarization ranging from -600 mV to ~ -300 mV (stop at 0.1 mA) in neutrally aerated 0.1 M NaCl solution at 25 °C. Before the experiments, the sample surface area of 0.785 cm^2 was exposed to the solution for 30 minutes, by which time a stable potential (open circuit potential) could be monitored. The electrochemical workstation by Sensortechnik Meinsberg GmbH has a conventional three-electrode set-up. A saturated calomel electrode (SCE) equipped with a Haber-Luggin capillary provides the reference potential. The platinum plate was used as counter electrode. As corrosion characteristics, the corrosion potential and corrosion density by extrapolating the Tafel lines and the pitting potential of each polarization curve were determined.

2.3. Wear behaviour

The resistance against abrasive as well as oscillating friction and wear were tested. For the first, the scratch test by CSM Instruments S.A. was selected. A Rockwell indenter with 200 μm in diameter scratched a 5-mm-long path at a constant load of 10 N (velocity: 2.48 mm min^{-1}, humidity: 45-50%, temperature: 22±2 °C). For calculating the material-dependent characteristic value of scratch energy density (*sed*), the following relation

$$sed = \frac{F_R}{A_1}\left[\mathrm{J\ mm^3}\right] \quad (1)$$

was used, where the friction load (F_R) and the cross-sectional area of the obtained scratch (A_1) are necessary. The higher the *sed*-value the more resistant against abrasion is the material or the surface of the material [10].

Scratch tests were realized in the extrusion direction and perpendicular to it to obtain the effect of anisotropy resulting from the fabrication. The oscillating friction behaviour was tested with the oscillating friction and wear test (SRV) by Optimol Instruments (Fig. 2) with a frequency of 20 Hz for a stroke of 1 mm and a load of 10 N being comparable with the scratch tests. The testing time was terminated restricted to 15 minutes. Humidity was adjusted between 45 and 50% at a room temperature of 22 ± 2 °C. For the determination of the mass loss and emerging wear volume, at least three measurements were considered. The latter was obtained optically by a 3D profilometer.

Hence, corrosion and wear characteristics were obtained by calculating the mean value of at least three measurements.

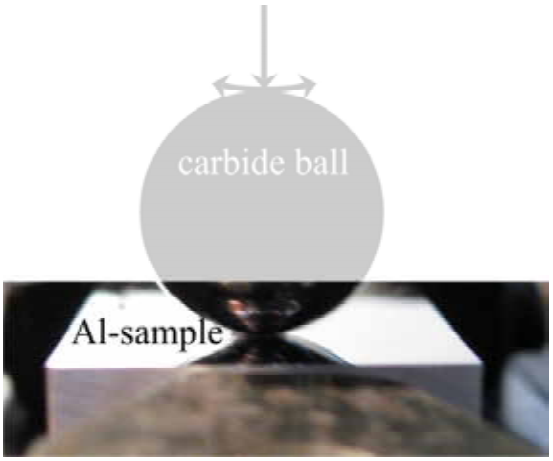

Fig. 2. Set-up of the ball-on-disc test consisting of the polished sample (base body) and a carbide ball with the chemical composition of WC6Co (calibrated according to DIN EN ISO 6506-2) as counterbody.

2.4. Microstructure

Before and after the corrosion experiments, the microstructure was studied by field emission scanning electron microscopy (FE-SEM ZEISS Neon40EsB). Phase and texture analyses were realized by X-ray diffraction experiments (Siemens D5000). Co radiation (tilting angle: $0° \leq \Delta\psi \geq 80°$, rotation angle: $0° \leq \Delta\varphi \geq 355°$ with a step size of 5°, respectively) was used for the determination of the texture, and Cu radiation (diffraction angle: $25° \leq \Delta\psi \geq 145°$ with a step size of 0.02°) for the analyses of the containing phases. The evaluation of the data measured for the texture was realized by Bruker AXS TEXEVAL software of the DIFFRACplus package. Owing to the similar texture of the different material conditions (Table 1), the sharpness of such preferred orientations can be compared using a quantitative value called texture index [11]. The software evaluation page EVA of the DIFFRACplus package by Bruker AXS was applied for the phase determination.

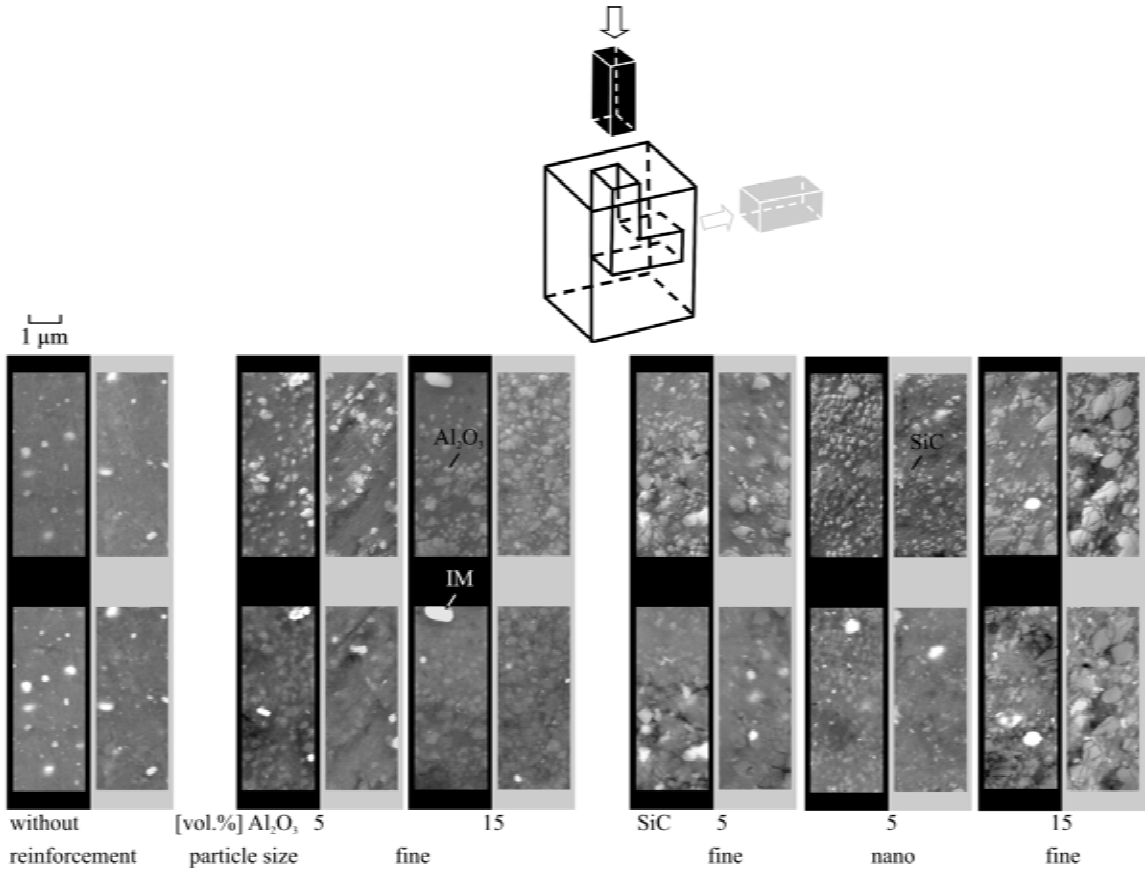

Fig. 3. SEM micrographs of the Al-Cu alloy without/with SiC/Al_2O_3 particles (secondary electron (upper) and backscattered electron (lower) images).

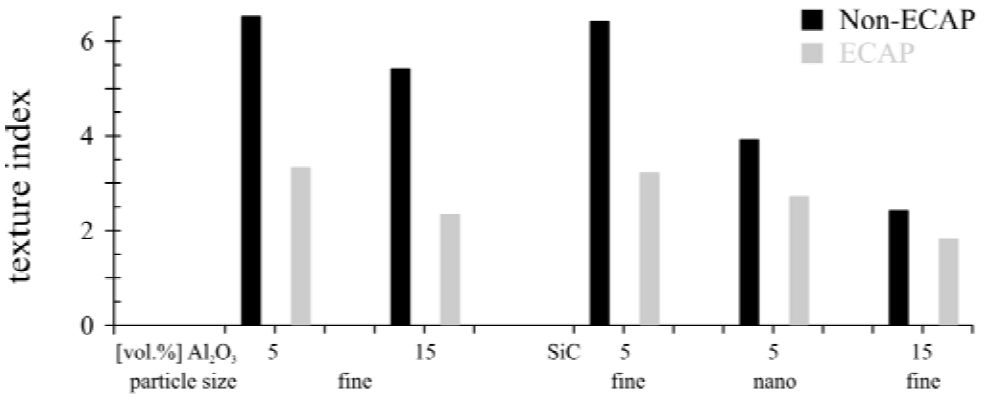

Fig. 4. Texture indexes of the composites with either Al_2O_3 or SiC particles.

3. RESULTS AND DISCUSSION

Fig. 3 exhibits the microstructure of the twelve investigated material conditions with differences in amount, size and type of reinforcement before and after the corresponding processing (Table 1). The very light appearing areas in the backscattered electron micrographs in Fig. 3 mark the iron-rich intermetallic phases (IM) with differing chemical compositions whereas the others are the reinforcement particles.

The fine SiC particles occur in the hexagonal modification, whereas the nanometre-scaled SiC is face-centred cubic. However, until now no effects on corrosion have been found which can be directly correlated with this difference in the lattice. The stable phase Al_2Cu was detectable by X-ray diffraction analysis just for the ECAP conditions containing 5 vol.% of nano-SiC and 15 vol.% of fine SiC particles. This fact can be attributed to the artificial (under-) aging before ECAP as well as to the elevated temperature during the ECAP process itself (promoting the stable Al_2Cu-phase) compared to the other material conditions (Table 1).

The influence of ECAP on the texture of the composites is summarized in Fig. 4. After processing, all aluminium matrix composites exhibit weaker, almost similar global textures in the considered extrusion plane with a $\langle 111 \rangle$ -fibre texture which is rotated by 45° correlating to the shearing (Figs. 5b and 5d). The initial (extruded) conditions show either a strong $\langle 111 \rangle$ - and weak $\langle 111 \rangle$ -double fibre texture (Fig. 5a) or a strong -single fibre texture (Fig. 5c).

The corrosion behaviour of the investigated materials is characterized by the corrosion potential similar to the corrosion resistance. The bar chart in Fig. 6 exhibits that the addition of particles for non-ECAP composites has just a slightly detrimental effect on the composites with Al_2O_3 and 5 vol.% SiC_{fine}. After ECAP, the non-reinforced materials and those reinforced with Al_2O_3 and 5 vol.% SiC_{fine} retain their corrosion potentials. On the contrary, ECAP at elevated temperatures leads to obviously reduced values, i.e. lower corrosion resistance. There is evidence that this behaviour correlates with the formation and growth of the stable intermetallic phase Al_2Cu originating from the thermal history before and during the ECAP process as proven by the XRD phase analysis. Therefore, the positive effect of fragmented and redistributed reinforced particles plays a secondary role compared to the multiphase alloys such as Al-Mg-Si [1]. The reason is seen in the different electrochemical potentials of Al_2Cu as well as SiC and Al_2O_3 in relation to the enclosing matrix phase, respectively.

In comparison with Fig. 7, it is obvious that the pitting potential for the presented material was close to the corrosion potential. Therefore, it is difficult to distinguish between these two corrosion characteristics which are not unusual for Al-Cu based alloys as well as composites. In consequence, as generally known, pitting occurs spontaneously without any passivity, i.e. the anodic current densities increase rapidly at the corrosion potential caused by the passive film breakdown and the associated onset of pitting.

The preferential sites for pits are always close to the precipitates or reinforcing particles, as shown in Fig. 8 owing to the above mentioned different corrosion behaviour of the adjoining materials. Their

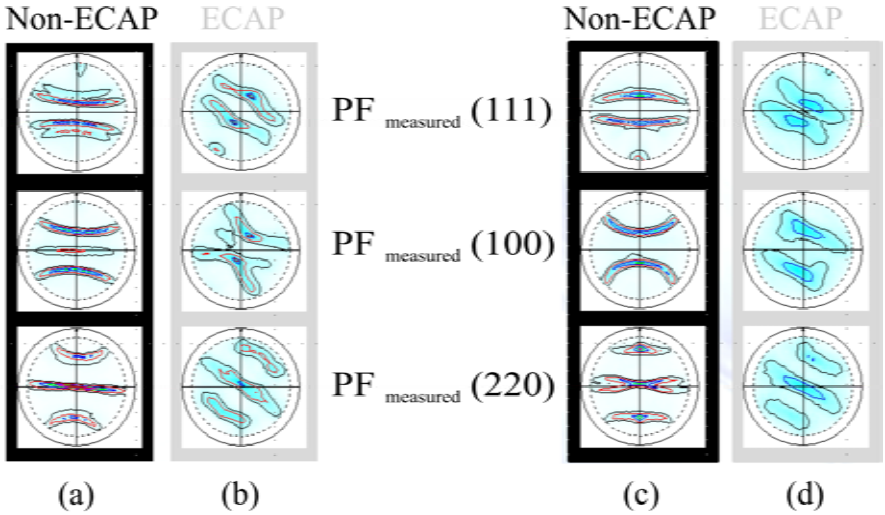

Fig. 5. Typical pole figures for (a) non-ECAP + 5% Al_2O_3 and non-ECAP 5% SiC_{fine}, (c) non-ECAP + 15% Al_2O_3, non-ECAP 5% SiC_{nano} and non-ECAP 15% SiC_{fine}, (b) and (d) for all ECAP composites after one ECAP pass.

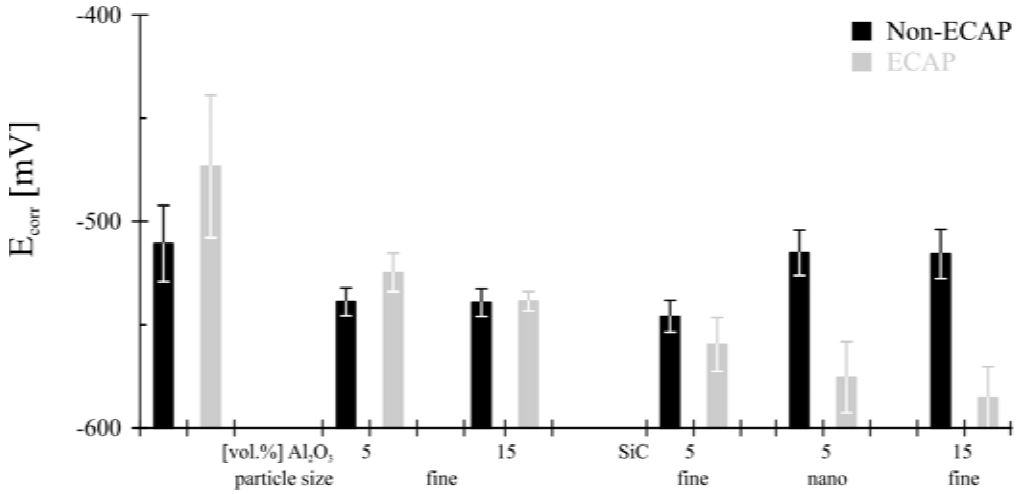

Fig. 6. The corrosion potentials E_{corr} as a function of the different material conditions.

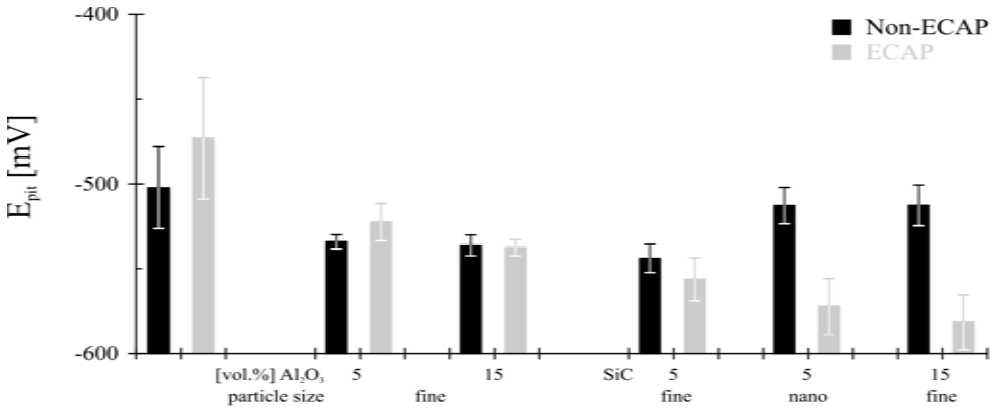

Fig. 7. The pitting potentials (E_{pit}) as a function of the different material conditions.

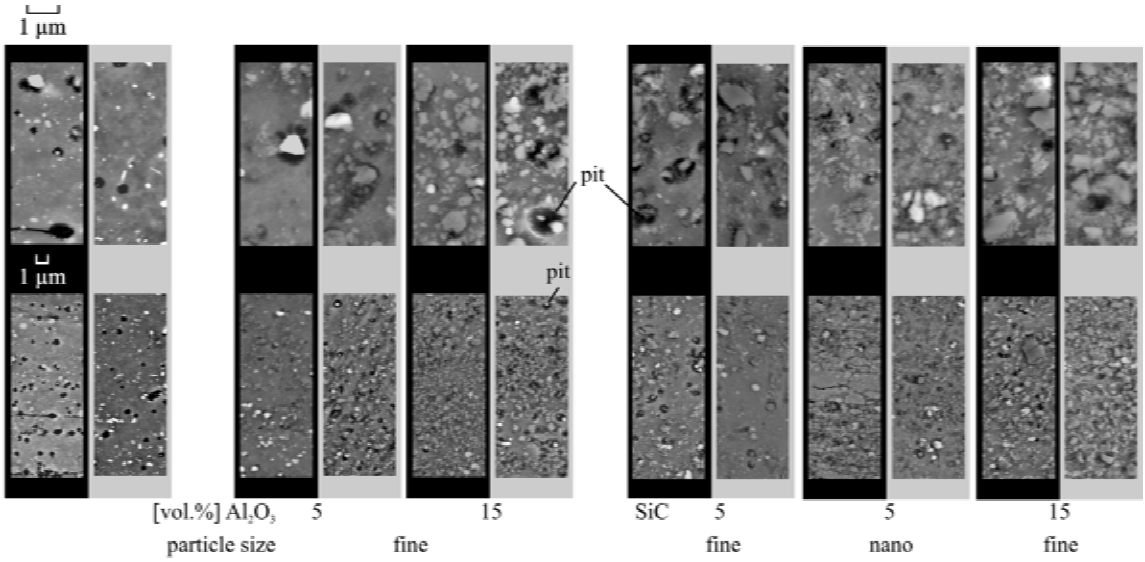

Fig. 8. SEM micrographs of the Al-Cu alloy without/with SiC/Al_2O_3 particles (secondary electron (upper) and backscattered electron (lower) images) after the corrosion damage.

appearance can be described as round as well as irregularly shaped. Pre-existing voids, crevices along the reinforcement and corrosion along the grain boundary can be found predominantly in the SiC composites. In contrast, the material with Al_2O_3 particles exhibits reinforced regions with fewer and narrower pits, whereas in the non-reinforced regions, the pits appear larger and rounder and located near precipitates. The inspection of the corrosion attack in Fig. 8, however, reveals no noticeable differences for the ECAP conditions compared to the non-ECAP conditions of the composites. The non-reinforced materials show smaller and fewer round pits after ECAP than the non-ECAP counterpart, which is consistent to the findings regarding the corrosion damage of other Al alloys such as Al-Mg-Si [1]. Nevertheless, further research is necessary, in particular to obtain quantified measurements about depth and extension of the corrosion pits.

Fig. 9 presents the results of the scratch energy density values received by scratch testing. As expected for composites, the addition of particles significantly increases the resistance against grooving of all particle-reinforced materials with the exception of the 5 vol.% SiC_{fine} condition. This abrasive resistance can be characterized as dominant abra-

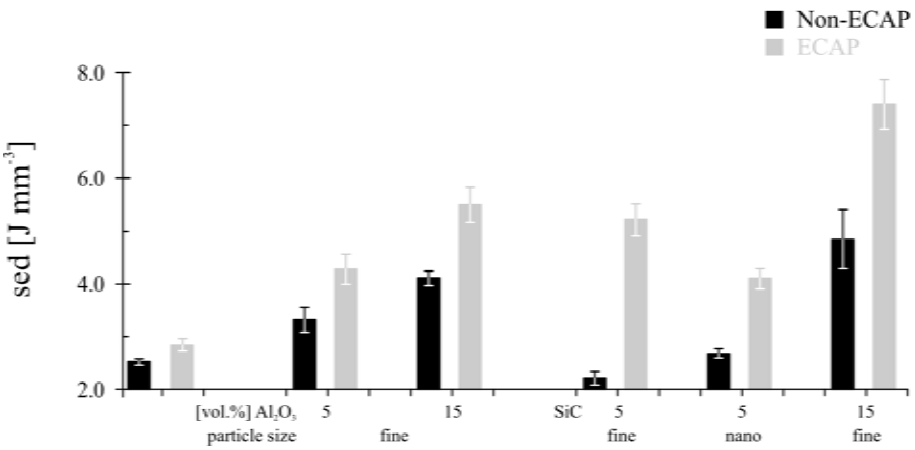

Fig. 9. Scratch energy density (sed) as a function of the different material conditions.

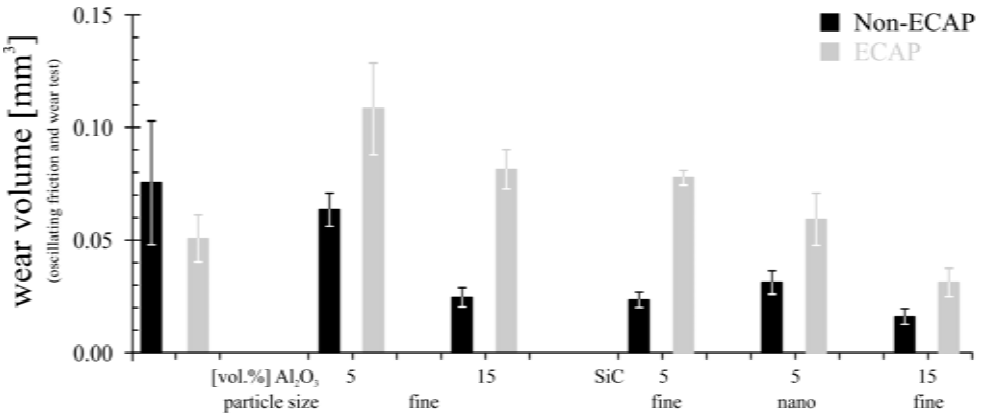

Fig. 10. Wear volume after oscillating friction and wear test determined optically by 3D profilometry as a function of the different material conditions.

sion wear mechanism. After one ECAP pass, this value increases further, which means that the ECAP material delivers higher wear resistance against abrasive loading compared to the non-ECAP condition of the same composition.

Furthermore, the material behaviour under another kind of wear loading was realized in the oscillating friction and wear tests. The corresponding results, summarized in Fig. 10, indicate the improved wear resistance of non-ECAP composites in general. They are in agreement with the results of the scratch tests described before. After just one ECAP pass, however, an opposite behaviour can be determined. The wear volume increases for all considered composites with the exception of the non-reinforced material. Under dry oscillating friction loading and the chosen tribological system (carbide as counterbody), the ECAP conditions seem to be a less suitable for repeated loading. It is assumed that this behaviour might be attributed to a reduced fatigue performance.

The material with 15 vol.% SiC in the non-ECAP and ECAP condition offers the most promising tribological behaviour for both wear loadings conducted.

4. CONCLUSIONS

The presented results represent the response to the required information concerning the influence of ECAP on the corrosion and wear characteristics of composites. After different thermomechanical treatments including ECAP-processing, a global texture weakening of the investigated composites with differences in type and size of the used reinforcements was observed. The presented study shows that there are no detrimental effects of room temperature ECAP on the corrosion behaviour of Al_2O_3- and SiC-reinforced composites compared to the non-ECAP and unreinforced counterparts. However, ECAP at elevated temperatures leads to lower corrosion susceptibility because of the formation and growth of an additional phase (Al_2Cu) which is important for the application.

Under different wear conditions, namely dry oscillating friction and wear as well as scratch tests, an opposite development can be stated: the abrasive wear resistance increases after one ECAP pass compared to the non-ECAP condition of the same composition; whereas the repeated loading of the composites leads to a former fatigue of the ECAP conditions regardless of which thermomechanical treatment. Non-reinforced materials exhibit no negative effect after ECAP. Hence, we suggest that the reinforcements are the weak points for this described tribological system. Further investigations including fatigue tests have to be done to clarify the decreased wear resistance of ECAP composites under dry-friction loading.

ACKNOWLEDGEMENTS

The authors gratefully acknowledge the Deutsche Forschungsgemeinschaft (DFG) for supporting this work carried out within the framework of the Collaborative Research Center 692. Technical assistance of D. Weißbach, G. Röllig, E. Benedix, C. Gläser and U. Faust is gratefully acknowledged.

REFERENCES

[1] B. Wielage, D. Nickel, T. Lampke, G. Alisch, H. Podlesak, S. Darwich and M. Hockauf // *Materials Science Forum* **584-586** (2008) 988.

[2] R.Z. Valiev and T.G. Langdon // *Progress in Materials Science* **51** (2006) 881.

[3] M. Hockauf, L. W. Meyer, D. Nickel, G. Alisch, T. Lampke, B. Wielage and L. Krüger // *Journal of Materials Science* **43** (2008) 7409.

[4] B.K. Prasad, K. Venkateswarlu, S. Das, A.K. Jha and R. Dasgupta // *Journal of Materials Science Letters* **16** (1997) 1113.

[5] K. U. Kainer, *Metallische Verbundwerkstoffe* (Wiley-VCH Verlag GmbH & Co.KGaA, Weinheim, 2003).

[6] J. R. Davis, *Corrosion of Aluminum and Aluminum Alloys* (ASM International, Cleveland, 1999).

[7] V.M. Segal // *Materials Science and Engineering A* **386** (2004) 269.

[8] M. Hockauf, L. W. Meyer and L. Krüger // *Materials Science Forum* **584-586** (2008) 685.

[9] H. Podlesak, S. Siebeck, S. Mücklich, M. Hockauf, L.W. Meyer and B. Wielage // *Mat.-wiss. u. Werkstofftech*. **40, 7** (2009) 500.

[10] B. Patzelt and U. Hemmann // *Materialwissenschaft und Werkstofftechnik* **28** (1997) 500.

[11] Bruker, *Diffrac^{plus} Basic Texeval - Texture Evaluation Program - user's manual* (Bruker AXS GmbH, Karlsruhe, 2006).